

# LOCAL PRESSURE FLUCTUATION AROUND A CAVITY SURFACE OF A HETEROGENEOUS NUCLEATION SITE

*Lilac Cuiling Wang, S. N. Leung, Markus Bussmann and Chul B. Park  
Department of Mechanical & Industrial Engineering, University of Toronto  
Toronto, Ontario, Canada M5S 3G8*

## Abstract

Heterogeneous nucleation in polymeric foaming processes forms at preferential sites such as phase boundaries or additives and requires less energy. Rough surfaces, especially cavities, on a processing wall or on additive particles are commonly found within a polymer-gas solution, and these are regions where cell nucleation can be initiated. In most previous studies on cell nucleation, a uniform pressure throughout the solution was assumed; and the discontinuity at the interfaces between the additives and surrounding material was neglected. A recent study [1] has shown that, the pressure and stress fields at discontinuities within a polymer-gas solution vary evidently from the surrounding areas due to the melt flow dynamic induced by the growth of nucleated bubbles; and regions at these discontinuities are the places where cells are propagated. However, the effect of surface geometry of an additive particle or the roughness of a processing wall, which is related to the underlying mechanisms of interfacial enhanced nucleation, has not studied. This paper presents a numerical analysis to investigate the pressure profile around a cavity surface inside a heterogeneous nucleation site. Such an investigation is expected to provide more insights to understand the cell nucleation phenomena.

## Introduction

Nucleation in polymer processing is defined as the process by which nuclei are formed. Nucleation can be subdivided into two types: homogeneous nucleation and heterogeneous nucleation. Homogeneous nucleation refers the formation of nuclei in the bulk of the material matrix without contacting any other foreign phase. Heterogeneous nucleation also involves two types: orientation-induced nucleation and additive-induced nucleation. Orientation-induced nucleation is a result of alignment of crystals (often due to process flow dynamics); while additive-induced heterogeneous nucleation involves the addition of a foreign phase presenting a new surface on which crystal growth can occur. Typically, this foreign phase takes the form of a nucleating agent.

Nucleating agents have long been employed in polymeric foaming processes to promote cell nucleation in order to increase cell density, reduce cell size, and improve cell uniformity. Such desirable cell morphology will translate into notable advantages in various applications, ranging from household products to advanced engineering applications. Comparing plastic foams to their solid counterparts, they can be customized to offer improved mechanical [2-3], thermal [4], acoustical [5], and optical properties [6]. Furthermore, the addition of nucleating agents can help to reduce the material usage, which typically accounts for 70% of the production cost of foam products.

The kinetics of nucleation depends on the thermodynamic driving force, which results from supersaturation; and pressure is a critical parameter that affects the degree of supersaturation within a polymer-gas solution. Nucleating agents, such as talc particles tend to aggregate together to form agglomerates [7]. Therefore, the surfaces of the heterogeneous nucleating sites are rough and can be modeled as a series of conical cavities, as indicated in Figure 1. Using the classical thermodynamics, it has been proven that the presence of heterogeneous nucleating sites of various shapes will help to reduce the free energy barrier to initiate cell nucleation [8-11], and thereby aid in generating more cells. This was the basis of various theoretical studies [12-18] of polymeric foaming processes over the past few decades. In these studies, researchers used the system pressure in the foaming equipment to approximate the pressure inside the polymer-gas solution during foaming processes, but this assumption ignored the local pressure fluctuation. Instead, it is believed that during a polymeric foaming process, either the local movement of the polymer-gas solution caused by the expansion of a nucleated bubble, or the flow of the polymer-gas solution around the rough surface will induce a stress field within the polymer matrix. The discontinuity between the nucleating agent and the surrounding polymer may lead to a local pressure field that is different from the bulk.

According to the classical nucleation theory [19-20], both the free energy barrier for heterogeneous nucleation ( $W_{\text{het}}$ ) and the critical radius for bubble nucleation ( $R_{\text{cr}}$ ) depend on the local pressure in the polymer matrix:

$$W_{het} = \frac{16\pi\gamma_{ig}^3 F(\theta_c, \beta)}{3(P_{bub,cr} - P_{sys})^2} \quad (1)$$

$$R_{cr} = \frac{2\gamma_{ig}}{P_{bub,cr} - P_{sys}} \quad (2)$$

where  $\gamma_{ig}$  is the surface tension at the polymer-gas interface;  $P_{bub,cr}$  is the pressure in a critical bubble; and  $P_{sys}$  is the local pressure in the polymer matrix;  $F$  is the ratio of the volume of the heterogeneously nucleated bubble to the volume of a spherical bubble having the same radius; parameters  $\theta_c$  and  $\beta$  are related to interfacial properties of a particle and the geometry of the particle respectively.

Pioneering studies [21-23] provided some qualitative insights into stress-induced cell nucleation. Lee proposed that the increase in cell density by adding nucleating agents might relate to the shear-induced nucleation [21]. Recent study by Leung *et al.* [24] demonstrated that the expansion of nucleated cells triggers the formation of new cells around them despite the lower gas concentrations in these regions. Wang *et al.* [1] also studied the effect of orientation-induced flow dynamics caused pressure differences between the bulk and local area around a nucleated bubble or additive particle. This paper presents a study of the local pressure fluctuation around a rough surface as on additive nucleating agents or on a processing wall. Eventually, it aims to provide new information about the underlying mechanism that promotes cell nucleation in the presence nucleating agents which possess rough surfaces.

In the following sections, a mathematical model based on the physical laws and assumptions is introduced; the numerical algorithm for solving the pressure field around a heterogeneous nucleating site is explained; and finally, several cases are studied and the simulation results are presented.

## Methodology

### Conservation Laws

The mixture of polymer melt and blowing agent consisting of nucleating agent particles is assumed to be a single-phase mixture, and the flow is assumed incompressible and steady state, if the particle does not move; the flow is assumed to be unsteady if the particle moves with the flow field or deforms due to the shear stress of the flow. The flow complies with conservation laws for mass and momentum, which are in the form of a set of partial differential equations:

$$\nabla \cdot u = 0 \quad (3)$$

$$\rho \frac{DU}{Dt} = \nabla \cdot \sigma + f \quad (4)$$

$u$  is the velocity vector,  $\sigma$  is the stress tensor,  $\rho$  is fluid density, and  $f$  is an external force term. The stress tensor is required to obey the constitutive equations:

$$\sigma = -PI + \tau \quad (5)$$

and

$$\tau = 2\mu(\dot{\gamma})d \quad (6)$$

where  $P$  is the fluid pressure,  $I$  is the identity tensor,  $\mu$  is the dynamic viscosity, and  $d$  is the rate-of deformation tensor given by:

$$d = \frac{1}{2}[(\nabla u) + (\nabla u)^T] \quad (7)$$

where  $\dot{\gamma}$  is the local shear rate defined by

$$\dot{\gamma} = \sqrt{2tr(d \cdot d)} \quad (8)$$

The polymer melt is modeled as a purely viscous fluid,

where the shear rate ( $\dot{\gamma}$ ) dependent viscosity of the melt is described by a power-law model:

$$\mu(\dot{\gamma}) = m(\dot{\gamma})^{n-1} e^{-b(T-T_b)} \quad (9)$$

where  $m$  is the consistency index (unit of  $Pa \cdot s^n$ ),  $b$  is a constant and  $n$  is the power-law index.

### Numerical Algorithm

A finite element solver for three-dimensional non-Newtonian fluid flow has been developed based on an existing finite element solver [26]. The governing equations (10) and (11) are spatially discretized using a Galerkin finite element approach in conjunction with P2-P1 tetrahedral Taylor-Hood elements. The unknown velocity and pressure fields are expressed in terms of the shape functions  $\phi_j$  and  $\psi_j$  and the nodal velocity and pressure values  $u_j$  and  $p_j$ :

$$u = \sum_{j=1}^N u_j \phi_j \quad (10)$$

$$p = \sum_{j=1}^{N_p} p_j \psi_j \quad (11)$$

where there are  $N = 10$  degrees of freedom for velocity (in each co-ordinate direction) and temperature, and  $N_p = 4$  degrees of freedom for pressure. Following a Galerkin spatial discretization, the governing equations are written in semi-discrete form as:

$$[M] \frac{d\{u\}}{dt} + [S]\{u\} + [L]^T \{p\} = \int_{\Gamma} (-pn + \frac{\partial u}{\partial n}) dS \quad (12)$$

$$[L]\{u\} = 0 \quad (13)$$

where  $\{u\}$  and  $\{p\}$  are the vectors of nodal velocity and pressure.  $[M]$ ,  $[S]$  and  $[L]$  are elemental matrices,  $S$  is the boundary of the elemental volume, and  $n$  is a normal vector.

## Results and Discussion

### 3D Geometry and material properties

First consider a cavity (small but still large enough to have a flow field inside) along a solid wall, with a polymer melt flow above the cavity, as depicted in Figure 2. Another case is a cavity on a small additive particle immersed in a volume of polymer melt, Figure 3. These geometries were spatially discretized using the commercial software ICFM-CFD [26], and then studied by numerical modeling the flow of a polymer melt in the geometries. The finite element meshes for the geometries depicted in Figures 2 and 3 are shown in Figures 4 and 5 respectively. Progressively refined meshes for each geometry were constructed to ensure that the simulation results were mesh-independent. The material considered in this study is Styron 685D polystyrene with a weight-average molecular weight of 315 000 g/mol. The zero shear viscosity and the fitted parameters for calculating viscosity of the PS and gas solution were adopted from [27]. The physical blowing agent is 99% pure CO<sub>2</sub> (Linde Gas). The nucleating agent is talc particle, Stellar 410 (Luzenac) having a plate shape. An isothermal condition was assumed. A summary of material data used for the calculations, and the operating conditions considered, are listed in Table 1.

#### Case I: Cavity in a solid wall Velocity field and validation

Figures 6 and 7 show the velocity fields of the polymer melt around a cavity in a solid wall. A validation was made for a steady axial flow of a power-law fluid flowing in a cylindrical tube with the power-law indexes equal to 0.1; 0.5; 0.8 and 1.0 respectively, to compare the numerical result with analytical solution. The comparison shows that the agreement between the analytical and numerical results is essentially perfect, Figure 8. The streamline traces in Figure 7 indicates that the melt revolves in the cavity which will make the pressure different from a smooth surface.

#### Pressure distribution around a cavity in a solid wall

The pressure field in and around the cavity is shown in Figure 9, which shows the polymer melt mixture flowing above the cavity generates a sharp pressure change at the edge (corner) of the cavity. This is because

the flow field encounters a significant change near the cavity, which makes it a potential nucleation site. The pressure change along line AA in Figure 9 was plotted; the effect of the flow rate on the pressure profile is shown in Figure 10. Two flow rates were considered for the polymer melt mixture above the cavity: one is relatively high, as for an extrusion condition; the other is very low, as for the batch foaming condition. Figure 10 indicates that as the flow rate increases, the pressure around the edge of the cavity also increases. The pressure distribution contours for both the high and low flow rate cases are similar because the same cavity is involved.

#### Effect of the cavity angle

The cavity angle can have an effect on pressure profile since melt flow may encounter more abrupt changes when the cavity angle becomes smaller. Therefore, the effect of the cavity angle on pressure field was investigated. The pressure profile along AA for different cavity angles  $\theta$  (sharp to wide,  $\theta = 30^\circ, 60^\circ, 90^\circ$ ) is plotted in Figure 11. It clearly shows that as the cavity angle becomes sharp, the pressure also changes dramatically, which indicates that a sharper cavity will be advantageous to cell nucleation.

#### Case II: Cavity on a particle surface

Consider a cavity on one surface of a hexahedral particle, which is immersed in the polymer gas solution as depicted in Figure 3. Simulations were performed for two cases, each of which has a different flow direction, to check the pressure profile around the cavity inside the particle. A specified flow rate, which represents the flow rate under batch foaming condition, was used for each case, and the particle sticks in a spot of the mixture. The pressure distribution in and around the cavity for each case are shown in Figure 12 and Figure 13 respectively. These results reveal that the polymer melt mixture flowing around the particle with a cavity surface generates dramatic pressure changes inside and around the cavity. The pressure changes along Line 1, 2 and 3 in Figure 13 were plotted in Figure 14 to show the details varieties of the pressure close to the cavity. Figure 14 indicates that pressure reaches two extreme values along the flow direction on the top and the bottom of the added particle, and this result is identical with the results as explained in [28]; pressure exhibits a distinct change around the cavity and more variation occurs close to the border of the cavity. Figure 15 compares the pressure distribution around a particle immersed in the mixture with smooth surfaces. The comparison indicates that more pressure fluctuation appears when a cavity presents on the surface of a particle, which results in a potential nucleation site.

## Conclusions

Pressure is an important parameter that affects cell nucleation. Knowledge of the pressure variation and distribution around a nucleation site is a key to understanding of the underlying mechanism that promotes cell nucleation. To highlight this, numerical simulations of the pressure profiles around nucleating sites in a mixture of polymer melt and blowing agent have been conducted. Several cases were studied and, the issues that affect pressure distribution were investigated. The presence of cavities on a processing wall and additive particles creates discontinuities in the foaming mixture. Cavities on a processing wall or on an additive particle cause distinct pressure fluctuation around the cavities, where the effective surface energy is lower, thus diminished the free energy barrier and facilitating nucleation. The geometry of a cavity has an effect on pressure distribution, and a cavity with a smaller conical angle induces bigger pressure fluctuation. Compared to a smooth surface additive particle, a particle with rough surfaces brings more change of nearby pressure fields, thereby promotes nucleation.

## Acknowledgments

The authors are grateful to the Ontario Centres of Excellence (OCE) and the Consortium for Cellular and Microcellular Plastics (CCMCP) at the University of Toronto for the financial support of this study.

**Keywords:** Nucleation, pressure fluctuation, nucleating agent, numerical simulation.

## References

1. Wang, L.C., Leung, S.N., Bussmann, M., and Park, C.B., "Numerical Investigation of Additive Particle - Enhanced Heterogeneous Nucleation", *Chemical Engineering Science* submitted, 2009.
2. D.F. Baldwin and N.P. Suh, *SPE-ANTEC Tech Papers*, 38, 1503 (1992). K.A. Seeler and V. Kumar, *ASME, Cellu. Polym.*, 38, 93 (1992).
3. K.A. Seeler and V. Kumar, *ASME, Cellu. Polym.*, 38, 93 (1992).
4. L. Glicksman, *Notes from MIT Sum Prog 4.10S Foam and Cellu. Mater: Therm. and Mech. Prop.*, Cambridge, MA, June 29-1 (1992).
5. K.W. Suh, C.P. Park, M.J. Maurer, M.H. Tusim, R.D. Genova, R. Broos, and D.P. Sophiea, *Adv Mater*, 12, 1779 (2000).
6. A. Kabumoto, N. Yoshida, M. Itoh, and M. Okada, US Patent 5844731 (1998).
7. J.H. Han, and C.D. Han, *J. Polym. Sci.*, 28, 743 (1990).
8. D. Turnbull, and B. Vonnegut, *Ind. Eng. Chem.*, 44, 1292 (1952).
9. N.H. Fletcher, *J. Chem. Phys.*, 29, 572 (1958).
10. N.H. Fletcher, *J. Chem. Phys.*, 31, 1136 (1959).
11. R. Cole, *Adv. Heat Trans.*, 10, 85 (1974).
12. J.G. Lee, and R.W. Flumerfelt, *J. Coll. Int. Sci.*, 184, 335 (1996).
13. M.A. Shafi, K. Joshi, and R.W. Flumerfelt, *Chem. Eng. Sci.*, 52, 635 (1997).
14. K. Joshi, J.G. Lee, M. Shafi, and R.W. Flumerfelt, *J. App. Polym. Sci.*, 67, 1353 (1998).
15. M. Shimoda, I. Tsujimura, M. Tanigaki, and M. Ohshima, *J. Cellu. Plast.*, 37, 517 (2001).
16. D. Mao, J.R. Edwards, and A. Harvey, *Chem. Eng. Sci.*, 61, 1836 (2006).
17. S.N. Leung, C.B. Park, and H. Li, *Plastics, Rubber and Composites: Macromolecular Engineering*, 35, 93 (2006).
18. Gibbs, J.W., *The Scientific Papers of J. Willard Gibbs*, Vol. 1; Dover: New York, 337 (1961).
19. Blander, M., and Katz, J. L., *AIChE J*, 21, 833 (1975).
20. L. Chen, H. Sheth, and X. Wang, *J. Celul. Plast.*, 37, 353 (2001).
21. S.T. Lee, *Polym. Eng. Sci.*, 33, 418 (1993).
22. L. Chen, H. Sheth, and X. Wang, *J. Celul. Plast.*, 37, 353 (2001).
23. C.Y. Gao, N.Q. Zhou, X.F. Peng, and P. Zhang, *Polym. Plast. Tech. Eng.*, 45, 1025 (2006).
24. Leung, S.N., Wong, A., Wang, C., and Park, C.B., "Elucidation of the Cell Nucleation Mechanism in Talc-Enhanced Polymeric Foaming Processes," *European Polymer Journal*, submitted, July 2009.
25. Mineev, P.; Ethier, C. A Characteristic/Finite Element Algorithm for Time Dependent 3-D Advection-Dominated Transport Using Unstructured Grids. *Computer Methods in Applied Mechanics and Engineering*, 2003, 192, 1281.
26. ICEM CFD engineering, ANSYS, Inc. ICEM CFD 5.0.
27. Lee M., Park C. B., and Tzogonakis C., *Polym. Eng. Sci.*, 39, 99 (1999)
28. Wang, L.C., Leung, S.N., Bussmann, M., and Park, C.B., "Finite Element Modeling of Pressure Profile Around a Particle Acting as a Heterogeneous Nucleation Site", *17th Annual Conference of the CFD Society of Canada*, Ottawa, Ontario, May 3-5, 2009.

**Table 1.** Material data and operating conditions

Parameters	Values
Density (g/ml)	0.910
CO <sub>2</sub> Content (wt%)	2.0
Power-Law Index ( <i>n</i> )	0.4
Power-Law Consistency ( <i>pa</i> • s <sup><i>n</i></sup> )	4000.0
Reynolds Number ( <i>Re</i> )	$1.0 \times 10^{-4}$
Flow-Rate (g/s)	20/0.2
Melt Temperature ( <i>T</i> )	180

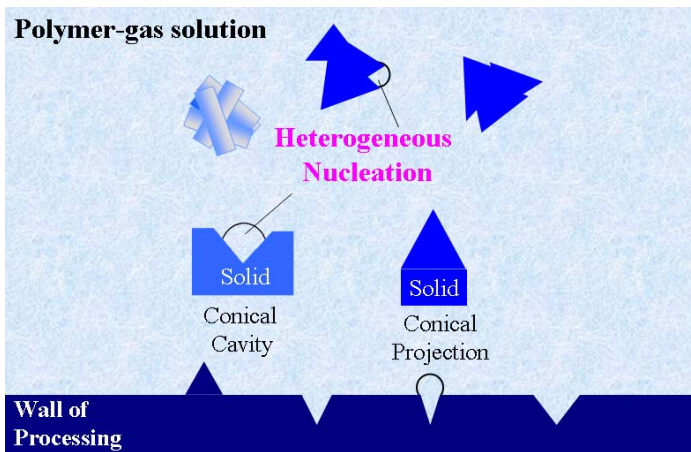


Figure 1. A schematic of a nucleation site

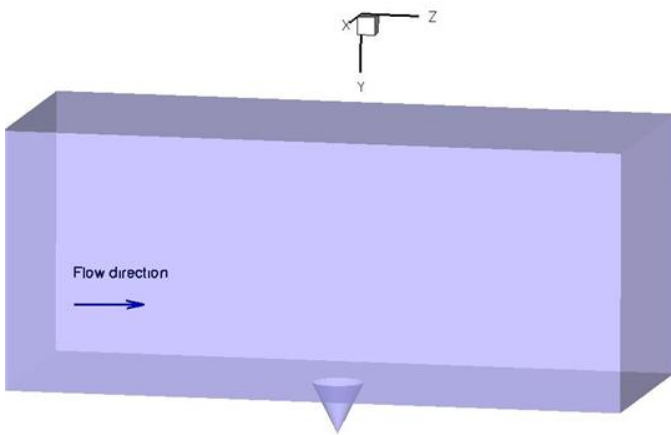


Figure 2. 3D geometry of a cavity on a processing wall

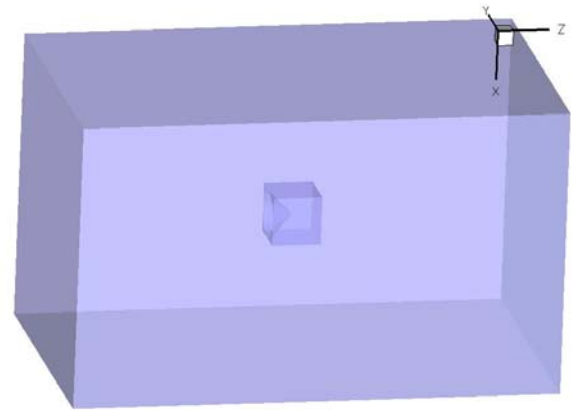


Figure 3. 3D geometry of a particle with a cavity on one of its surfaces immersed in a volume of solution

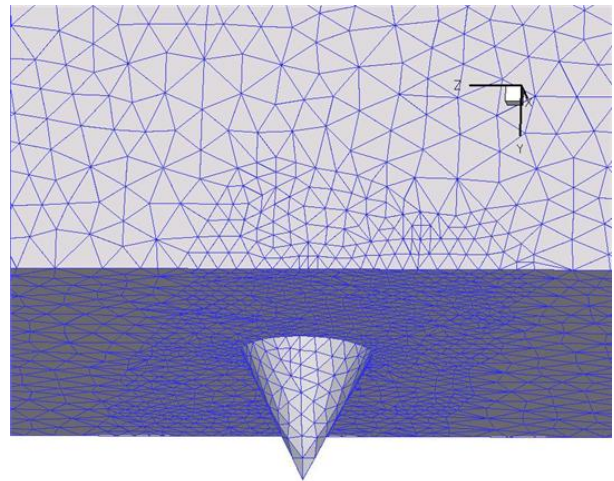


Figure 4. 3D Mesh for a cavity on a processing wall

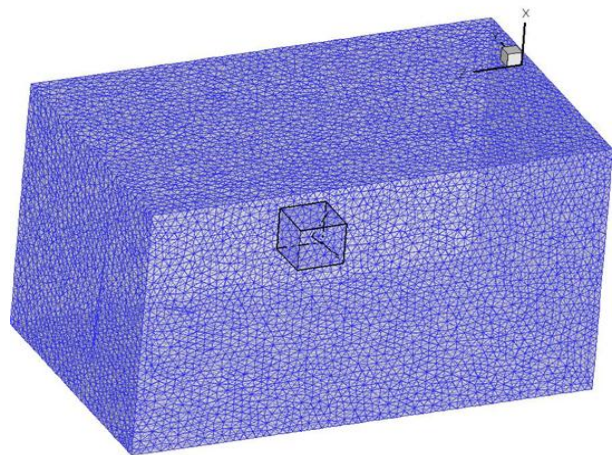


Figure 5. 3D Mesh for a cavity on a particle surface

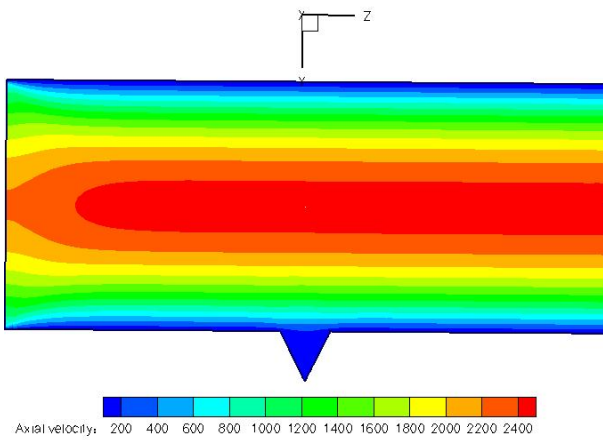


Figure 6. Velocity contour

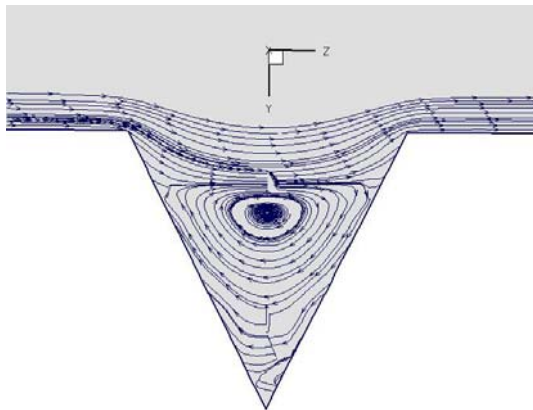


Figure 7. Streamline trace in the cavity of the processing wall

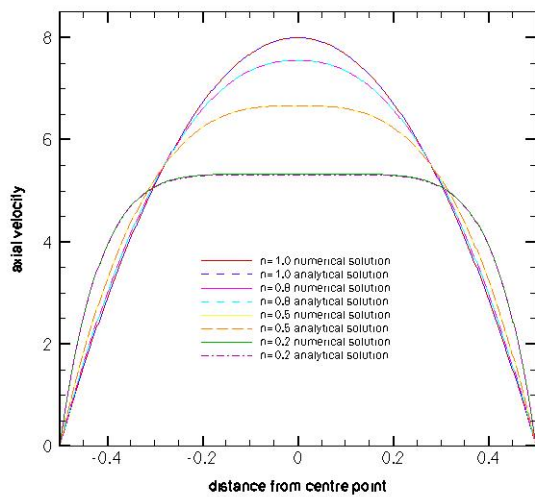


Figure 8. Validation: a comparison with analytical solution

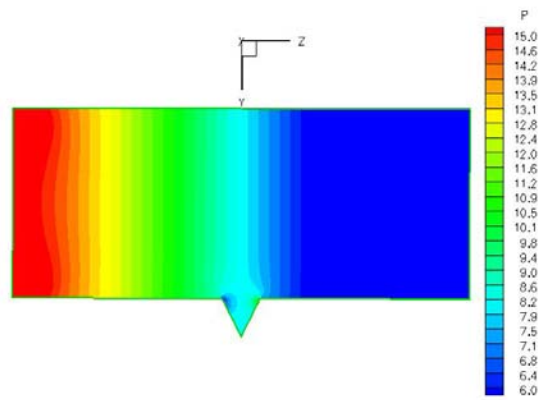


Figure 9. Pressure profile around the cavity in a processing wall

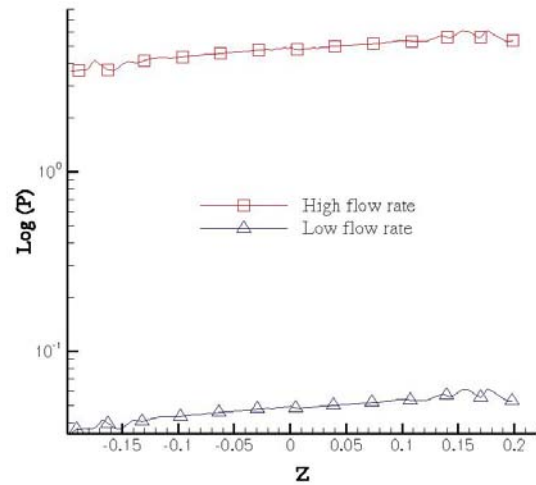


Figure 10. Effect of the flow rate on pressure distribution

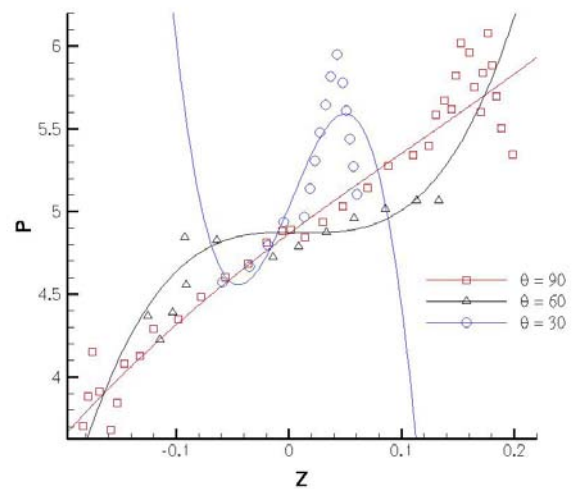


Figure 11. Effect of conical angle on pressure profile

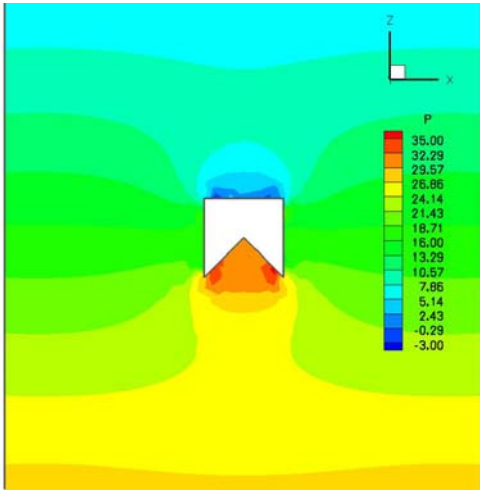


Figure 12. Pressure profile around a plate particle with a cavity on one of its surfaces

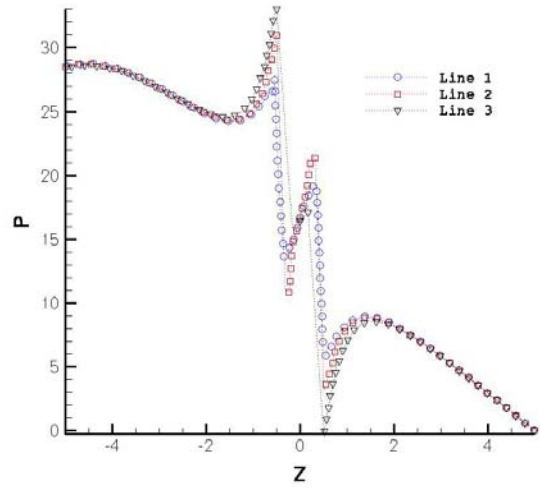


Figure 14. Pressure plot along lines in Figure 13

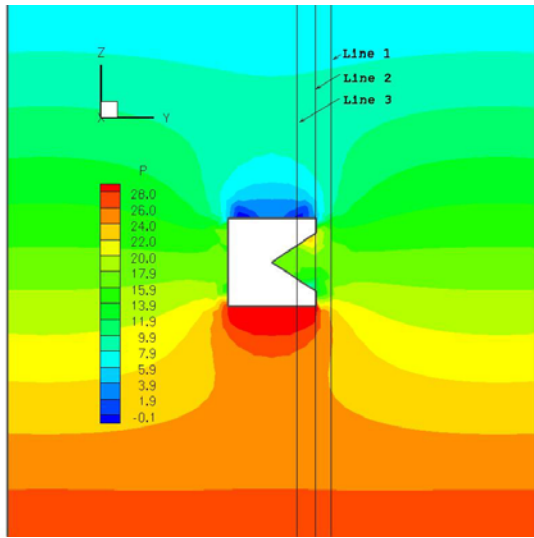


Figure 13. Pressure profile when flow direction has been changed

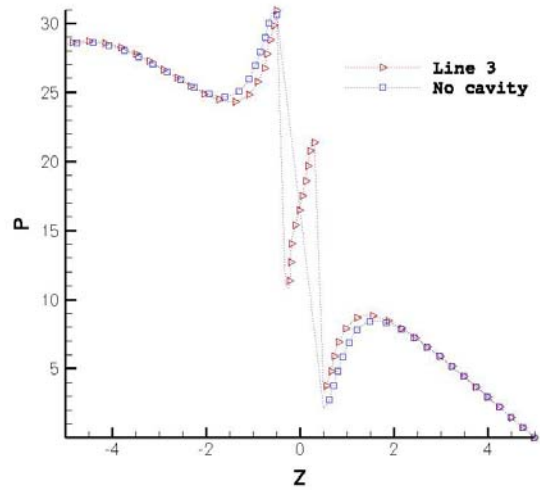


Figure 15. The effect of particle smoothness on pressure distribution